Feasibility study of heavy ion beam probe in CFQS quasi-axisymmetric stellarator

A. Shimizu[a,b], M. Isobe[a,b], S. Okamura[a], S. Kinoshita[a], K. Ogawa[a,b], H. Takahashi[a,b], T. Oishi[a,b], Y. Yoshimura[a], T. Murase[a], S. Nakagawa[a], H. Tanoue[a], H. Takubo[a], M. Osakabe[a,b], H. Hayashi[a], S. Kobayashi[a], H. F. Liu[c] and Y. Xu[c]

[a] *National Institute for Fusion Science, National Institutes of Natural Sciences, 322-6 Oroshi, Toki, Gifu 509-5292, Japan*
[b] *The Graduate University for Advanced Studies, SOKENDAI, 322-6 Oroshi, Toki, Gifu 509-5292, Japan*
[c] *Institute of Fusion Science, School of Physical Science and Technology, Southwest Jiaotong University, 111 N 1st Section, 2nd Ring Rd, Sha Xi Mei Shi Yi Tiao Jie, Jinniu District, Chengdu 610031, Sichuan, China*

E-mail: shimizu.akihiro@nifs.ac.jp

ABSTRACT: The world’s first quasi-axisymmetric stellarator, CFQS, is now under construction. The CFQS will be dedicated to studies on the interaction between flow and turbulence, and confinement improvement by suppression of turbulence in connection with proof-of-principle experiment of quasi-axisymmetry. In order to conduct this experimental research, a heavy ion beam probe (HIBP) system is planned to be installed and utilized to measure the radial electric field and its fluctuation in a CFQS plasma. In this paper, an orbit calculation for a probe beam is performed to verify feasibility of the HIBP in the CFQS. The required beam energy, possible ion species, and the observable region in a CFQS plasma are investigated. The beam attenuation by a CFQS plasma is also estimated for different beam ion species. If we use $^{133}Cs^{+}$ as a primary probe beam, the required beam energy is expected to be 30 ~ 50 keV, which is relatively easy to handle. In this case the beam attenuation, evaluated by the ratio between the injected and detected beam currents, is 10^{-3} ~ 10^{-2} in a CFQS plasma with a line-averaged electron density of $< 1.0 \times 10^{19}$ m^{-3}. For a higher density plasma, usage of $^{85}Rb^{+}$ is better in terms of low-beam-attenuation, and a high signal-to-noise ratio. The HIBP in the CFQS will provide a great opportunity to study physics experimentally, related to the radial electric field, poloidal flow, and turbulence suppression.

KEYWORDS: Advanced stellarator; Quasi-axisymmetry; CFQS; HIBP.

Contents

1. Introduction

In a magnetically confined fusion plasma, the radial electric field is one of the key physics parameters, since it plays an important role in its confinement property. The radial electric field (E_r) is strongly correlated to poloidal flow through $E \times B$ drift, and the shear flow tends to drive confinement improvement like H-mode [1-3] and/or the internal transport barrier [4-5] by suppressing turbulence transport. Recently, zonal flow is also a topic drawing attention, because the coupling between zonal flow and turbulence, which shows behavior like a predator-prey model, is important to obtain deeper understanding of confinement characteristics of a toroidal plasma [6-7]. Therefore, the measurement of E_r is crucial to investigate confinement physics and to explore the confinement improvement regime. A heavy ion beam probe (HIBP) [8] is a powerful diagnostic tool to study the physics related to E_r, because it can measure the potential, the electron density, the magnetic field, and their fluctuations in magnetically confined high temperature plasmas with high temporal and spatial resolutions, without causing any disturbances to a plasma of interest. Up to now the HIBP has been employed to investigate phenomena related to E_r and flow in various devices, for example, in tandem mirror devices[9, 10], compact/medium size tokamaks [11-14], and reversed field pinches [15], in which attractive physics such as the H-mode transition is studied with the HIBP. It was also installed in various stellarator/helical devices [16-21], in which control of the probe beam is more complicated than in the above devices, because the distance in the toroidal direction between ports for beam injection and ejection becomes larger, due to its three-dimensional (3-D) magnetic field structure. An appropriate probe beam control system has been designed to apply the HIBP to these stellarator/helical devices.

The quasi-axisymmetric stellarator CFQS was designed based on the CHS-qa [22-25], and is now under construction under a joint project of the National Institute for Fusion Science, Japan and Southwest Jiaotong University, China [26-30]. The CFQS magnetic configuration is characterized by low toroidal viscosity like that of a tokamak. Therefore a large plasma flow is expected and its interaction with turbulence will be important to improve confinement. Since the HIBP has very suitable features to study these physics, a feasibility study of this diagnostic is performed in this work. The CFQS magnetic field configuration has intrinsically a 3-D structure; therefore, we need to carefully survey the appropriate probe beam orbit and injection/ejection ports for the HIBP. In this paper, results of the feasibility study of the HIBP in the CFQS, i.e. probe beam orbit, arrangement of diagnostics ports, beam ion species, and acceleration voltage suitable for the CFQS are described.

2. Required energy for the probe beam in CFQS

The CFQS is a quasi-axisymmetric stellarator with a major radius of 1.0 m, an averaged plasma minor radius (a_p) of 0.25 m, and a toroidal magnetic field strength (B_t) of 1.0 T. The magnetic field is produced by 16 modular coils (MCs), designed by the NESCOIL code [31]. A schematic view of the CFQS is shown in Fig. 1, and the CFQS vacuum vessel is shown in Fig. 2, which has 46 ports for heating and diagnostic systems. Two large rectangular ports will be utilized for neutral beam injection heating and a Thomson scattering diagnostic. We need to use two ports for the HIBP, i.e., the top port with a ConFlat (CF) flange size of 203 mm in outer diameter for a probe beam injector, and the side port with a CF flange size of 305 mm in outer diameter for an energy analyzer and detector. For a probe beam of the HIBP, the Larmor radius of charged beam particles should be larger than the averaged plasma minor radius, in order to inject the beam into the plasma center. The Larmor radii, as a function of beam energy (E_b), are shown in Fig. 3. In the CFQS, ^{7}Li, ^{23}Na, ^{39}K, ^{85}Rb, and ^{133}Cs in single charge states are strong candidates as probe beam particles. Since a_p of a CFQS plasma is 0.25 m, at least E_b of 25 keV for $^{133}Cs^{+}$ is required. For other species, $^{7}Li^{+}$: 475 keV, $^{23}Na^{+}$: 145 keV, $^{39}K^{+}$: 85 keV, $^{85}Rb^{+}$: 39 keV are required as a minimum. Because we will reuse the high-voltage power supply (< 200 kV) of the HIBP used in the CHS [4, 16], $^{39}K^{+}$, $^{85}Rb^{+}$, and $^{133}Cs^{+}$ are acceptable from the viewpoint of probe E_b. However, E_b is necessary for $^{7}Li^{+}$ and $^{23}Na^{+}$ is over the ability of the high-voltage power supply utilized in the CHS. In the calculation of probe beam orbit, $^{133}Cs^{+}$ is assumed to be the strongest candidate as a primary beam ion species in this paper. Note that we can transform the required E_b for other species by multiplying the mass ratio between ^{133}Cs and the other beam ion species.

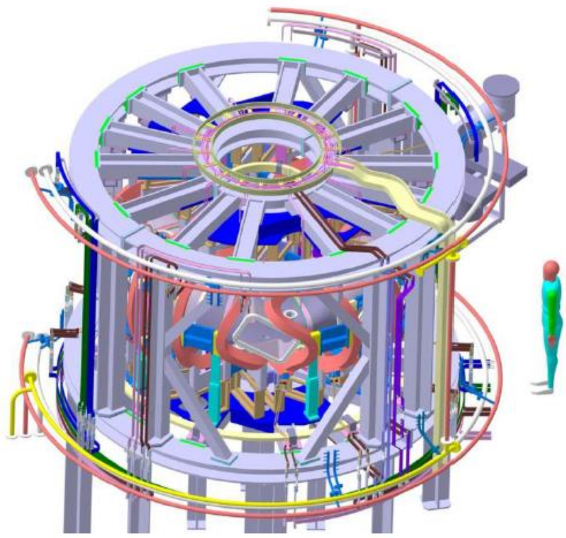

Figure 1. Three-dimensional computer-aided drawing of CFQS.

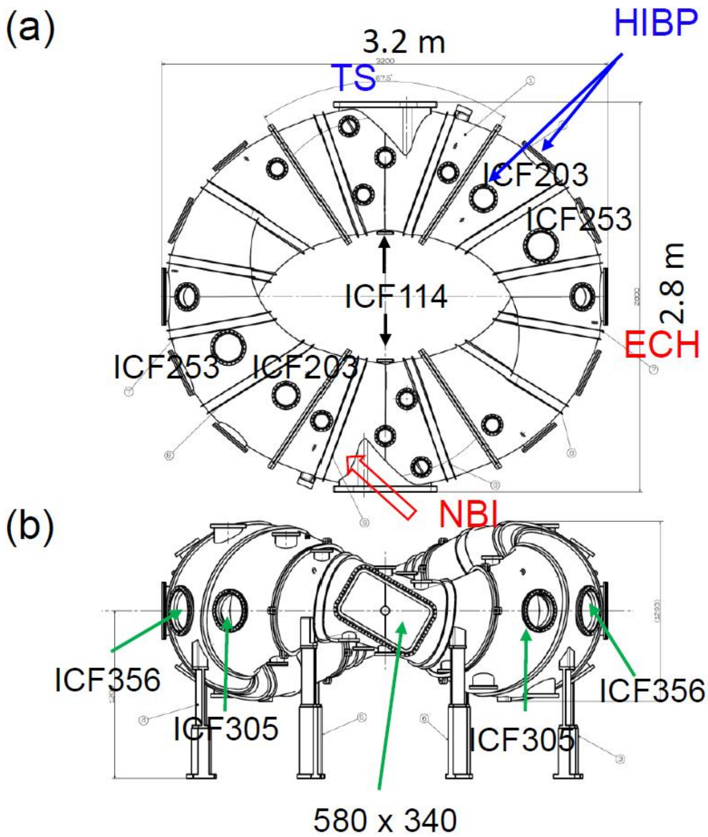

Figure 2. Vacuum vessel and port arrangement for CFQS. (a) top and (b) side view. TS represents Thomson scattering diagnostic. ECH and NBI stand for electron cyclotron resonance heating and neutral beam injection, respectively. ICF is designation of CF vacuum flange in Japan.

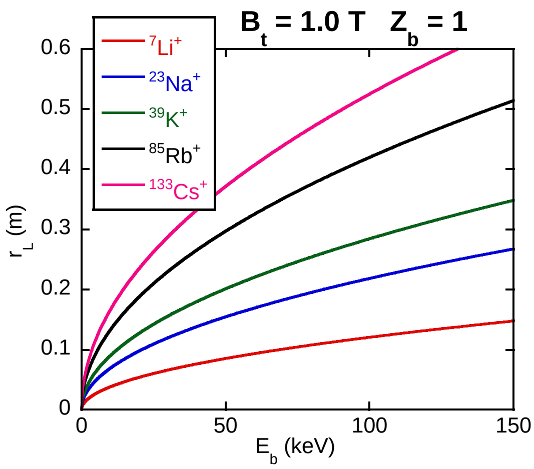

Figure 3. Larmor radius (*r_L*) as function of beam acceleration voltage (*E_b*) for various beam ion species on condition of magnetic field strength 1.0 T.

3. Beam orbit calculation results

In order to investigate the feasibility of the HIBP in the CFQS, probe beam orbits are analyzed. As a beam ion species, a single charged ^{133}Cs is selected. In the plasma, $^{133}Cs^{+}$ as a primary beam is changed to a secondary beam of doubly charged ion $^{133}Cs^{2+}$ by a collision with an electron of background plasma. The secondary beam coming out of the plasma is detected, and analyzed by an energy analyzer. From the energy conservation law, the local potential in a plasma can be measured by the difference of kinetic energy between the primary and secondary beam.

In the orbit calculation, the 3-D magnetic field of the CFQS, which is calculated by Biot-Savart's law from single filament coil data of MCs, is utilized. The detailed structure of the HIBP system, e.g. an 8-pole electrostatic sweeper [16] and energy analyzer, is not included. However, results shown here are meaningful in determination of the actual arrangement of those components. The injection point of the probe beam is chosen to be the center of the top port for simplicity, as an initial condition for the probe beam. For an energy analyzer, we will use the standard Proca and Green type of analyzer [32], therefore, the beam angle at the entrance of the energy analyzer is important. To adjust the beam angle there, we set a beam sweeper to control the beam angle by an electrostatic field in front of the energy analyzer. A detailed structure of the 8-pole electrostatic sweeper is not taken into account in this calculation. However, in the sweeper region, a uniform electric field, which is normal to the line of sight of the energy analyzer, is included and optimized. The electric field, $\boldsymbol{E}$, produced in the sweeper is characterized by two parameters, E_h and E_v, which are the horizontal and vertical components of $\boldsymbol{E}$ in the sweeper region. It is noted that $\boldsymbol{E}$ is almost normal to beam orbit, therefore, the E_b is not changed by this field.

The energy analyzer position is selected from a preliminary orbit calculation, in which the $\boldsymbol{E}$ in the sweeper region is not included. The position of the entrance of the energy analyzer is set at a point 0.25 m away from the port center of the CFQS vacuum chamber. The line of sight of the energy analyzer is adjusted to obtain a probe beam with an appropriate angle on the condition of $\boldsymbol{E} = 0$. The sweeper region is located between the outside port center, and a point 0.2 m apart from it. In Fig. 4(b), a detailed arrangement of the position for the entrance of energy analyzer, and the sweeper region is shown.

The beam injected from the center of injection port should reach the entrance of the energy analyzer with an appropriate angle. Therefore, with beam injection angles in the toroidal and poloidal direction at the injection point, two components of the electric field in the sweeper region, i.e., E_h and E_v, have to be optimized. In this process, we perform the iteration by using the following matrix,

$$\begin{pmatrix} \frac{\partial X_D}{\partial \theta} & \frac{\partial X_D}{\partial \zeta} & \frac{\partial X_D}{\partial E_v} & \frac{\partial X_D}{\partial E_h} \\ \frac{\partial Z_D}{\partial \theta} & \frac{\partial Z_D}{\partial \zeta} & \frac{\partial Z_D}{\partial E_v} & \frac{\partial Z_D}{\partial E_h} \\ \frac{\partial \alpha}{\partial \theta} & \frac{\partial \alpha}{\partial \zeta} & \frac{\partial \alpha}{\partial E_v} & \frac{\partial \alpha}{\partial E_h} \\ \frac{\partial \beta}{\partial \theta} & \frac{\partial \beta}{\partial \zeta} & \frac{\partial \beta}{\partial E_v} & \frac{\partial \beta}{\partial E_h} \end{pmatrix} \begin{pmatrix} \Delta\theta \\ \Delta\zeta \\ \Delta E_v \\ \Delta E_h \end{pmatrix} = \begin{pmatrix} \Delta X_D \\ \Delta Z_D \\ \Delta\alpha \\ \Delta\beta \end{pmatrix}. \qquad (1)$$

Here, θ, ζ, are injection angles in poloidal and toroidal directions, respectively, and X_D, Z_D are the horizontal and vertical position of the secondary beam on the virtual plane at the entrance of the energy analyzer, respectively. α, β are angles between beam and the line of sight of the energy analyzer at its entrance, in horizontal and vertical directions, respectively. (X_D, Z_D) = (0,0) means the position of the entrance of the energy analyzer. By using the inverse matrix of Eq. (1), the iteration calculation is carried out. Appropriate injection angles, θ, ζ, and two components of the electric field in the sweeper region, E_h, E_v, are obtained so that the secondary beam should reach the point of (X_D, Z_D) = (0,0) with a beam angle of (α, β) = (0,0). This iteration method is similar to that described in Refs. [16, 33]. A typical obtained orbit with E_b of 45 keV is shown in Fig. 4. Projections of the orbit on the top view plane (Fig. 4(a)) and on a poloidal cross section plane at a toroidal angle of 45 degrees (Fig. 4(b)) are shown. In Fig. 4 (b), the sweeper region, in which E_h and E_v are applied, is depicted. It is noted that the actual beam orbit has 3-D geometry. In Fig. 5, the probe beam in the 3-D CAD model, together with the CFQS vacuum vessel, are shown. In this case, both primary and secondary beams pass through the top and outside ports appropriately.

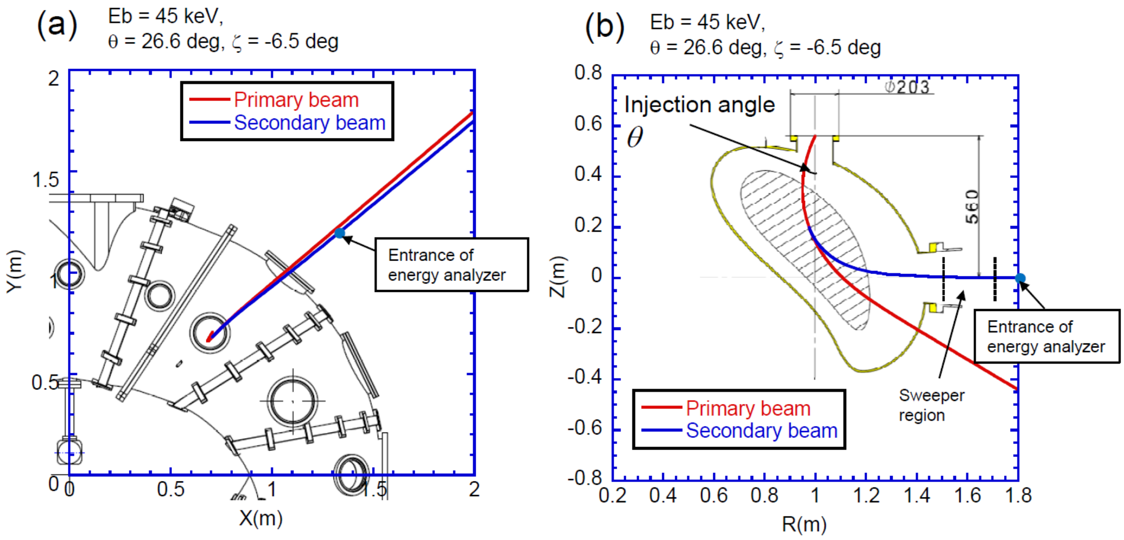

Figure 4. Example of probe beam orbit projected on (a) top view and (b) poloidal cross section plane. Orbit of $^{133}Cs^+$ with E_b of 45 keV is shown.

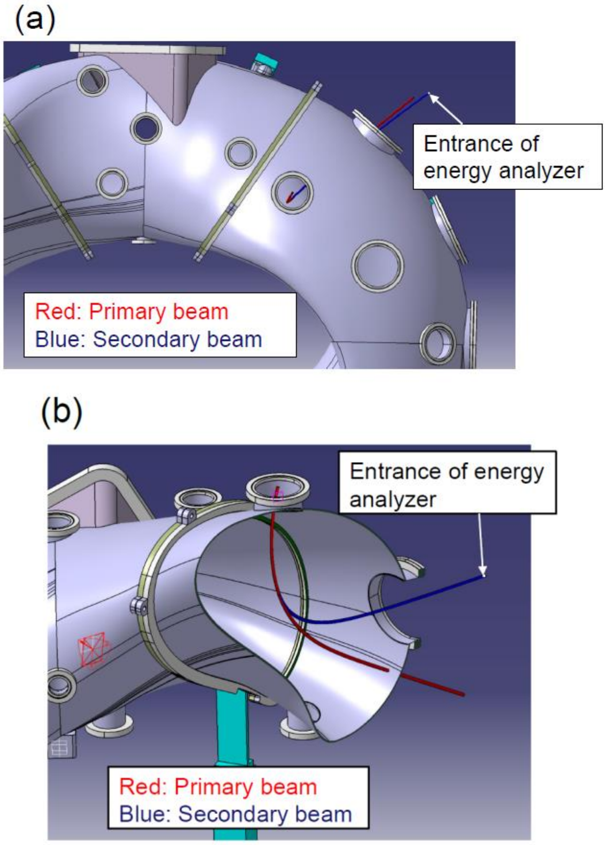

Figure 5. Example of probe beam orbit in 3-D CAD model with CFQS vacuum vessel. (a) top view and (b) poloidal view.

By scanning E_b and the injection angle, the observation region was calculated as shown in Fig. 6. For $^{133}Cs^+$, E_b of 30 ~ 50 keV are useful for the HIBP, which corresponds to the energy of $^{7}Li^+$: 570 ~ 950 keV, $^{23}Na^+$: 173 ~ 289 KeV, $^{39}K^+$: 102 ~ 171 KeV, and $^{85}Rb^+$: 47 ~ 78 keV. The range of injection angle in poloidal direction, θ, is from 10 to 50 degrees. When E_b is 40 keV for $^{133}Cs^+$, whole range of plasma minor radius can be measured.

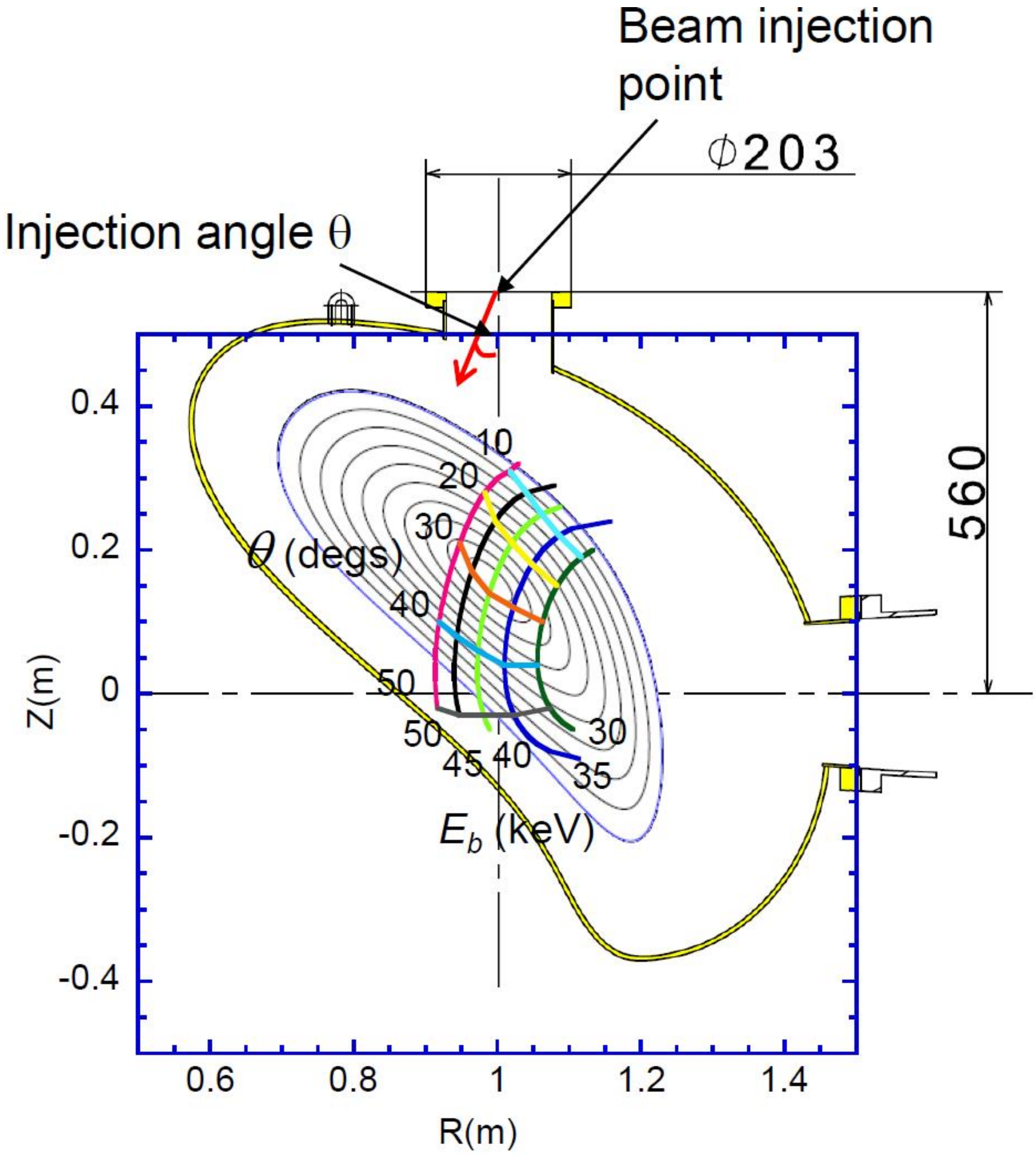

Figure 6. Observable region for $^{133}Cs^{+}$ when E_b is scanned from 30 to 50 keV. θ is the beam injection angle in poloidal direction.

4. Probe beam attenuation

For the HIBP, probe beam attenuation by collision with a plasma is an important factor to examine the appropriate density range in measurements for each probe beam species. The probe beam is attenuated mainly by collisions with electrons. The detected beam current of the secondary beam at the detector can be expressed as,

$$I_D = 2I_0 n_e \langle \sigma_1 v_e \rangle w / v_B \times \exp\left[-\int n_e \langle \sigma_1 v_e \rangle / v_B \, d\ell - \int n_e \langle \sigma_2 v_e \rangle / v_B \, d\ell \right]. \quad (2)$$

Here, I_0 is the injected current as the primary beam, I_D the detected current as the secondary beam, the $<\sigma_1 v_e>$ rate coefficient of $A^+ \rightarrow A^{2+}$ with electron impact, the $<\sigma_2 v_e>$ rate coefficient of $A^{2+} \rightarrow A^{3+}$ with electron impact, n_e the electron density, w the sample volume length, v_B the beam velocity, and dl the path integral along the beam orbit. The $^{133}Cs^+$ orbit shown in Fig. 4 is chosen to estimate I_D. For w, we assume it as 3 mm, which is reasonable for a slit size at the entrance of the energy analyzer. We use the rate coefficient estimated from Lotz's empirical formula [34], which as a function of electron temperature is shown in Fig. 7.The Lotz's empirical formula is expressed as follows,

$$\langle \sigma v_e \rangle = 3.0 \times 10^{-6} \sum_{i=1}^{N} \frac{q_i}{T_e^{1/2} P_i} \int_{P_i/T_e}^{\infty} \frac{\exp[-x]}{x} dx \ \ (\mathrm{cm}^3/\mathrm{s}) \,. \quad (3)$$

.

Here, $\langle \sigma v_e \rangle$ (cm^3/s) is the rate coefficient for a Maxwellian electron distribution of temperature T_e (eV). q_i is the number of equivalent electrons in the i-th subshell. P_i (eV) is the ionization potential.

Electron temperature and density profiles of a target plasma are assumed as, T_{e0} (1 - ρ^2), n_{e0} (1 - 0.8 ρ^2 + 1.3 ρ^4 - 1.5 ρ^6), and T_{e0} = 1 keV. Here, ρ represents a normalized plasma minor radius. In this case, the estimated value of I_D/I_0, as a function of the line-averaged electron density($\bar{n}_e$), is shown for $^{133}Cs^+$, $^{85}Rb^+$, $^{39}K^+$, $^{23}Na^+$ in Fig. 8. In these cases, E_b for each beam ion is as follows: 45 keV for $^{133}Cs^+$, 70.4 keV for $^{85}Rb^+$, 153.5 keV $^{39}K^+$, and 260.2 keV for $^{23}Na^+$. When $\bar{n}_e < 1.0 \times 10^{19}$ m^{-3}, ^{133}Cs is the best while in a range of $\bar{n}_e > 1.0 \times 10^{19}$ m^{-3}, $^{85}Rb^+$ is better for our purpose. For much higher density, $^{39}K^+$ is another possible option. From CHS experiments, when I_D is larger than a few hundred nA, a large signal-to-noise ratio can be achieved to measure turbulence and zonal flow in a plasma. Since I_D/I_0 ranges from 10^{-3} to 10^{-2}, as can be seen in Fig. 8, the primary beam current I_0 of a few hundred μA is required. This range of current is achievable by a zeolite ion source [35]. Therefore, the HIBP in the CFQS will provide a great opportunity to study attractive physics related to E_r with a sufficient signal-to-noise ratio.

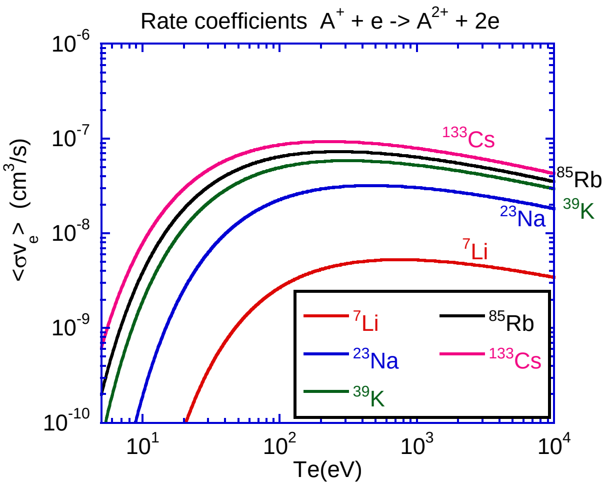

Figure 7. Collision rate coefficients of $A^+ \rightarrow A^{2+}$ for various beam ion species by the electron impact as a function of T_e.

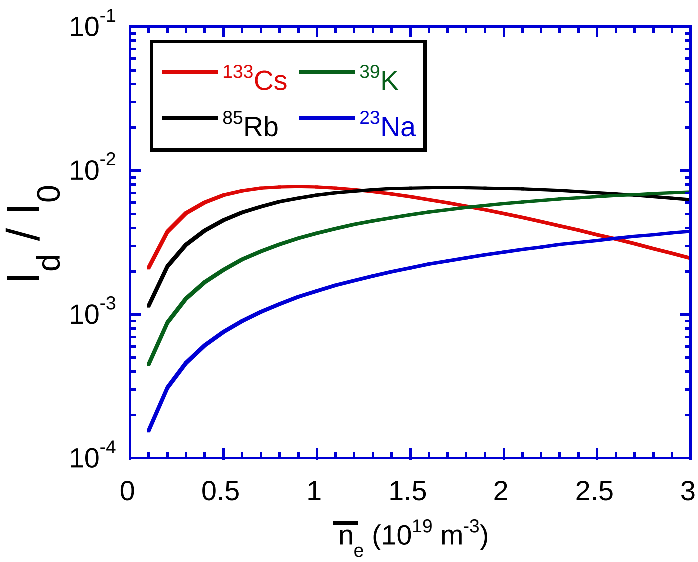

Figure 8. Beam attenuation of I_D/I_0 as a function of line-averaged electron density for various beam ion species.

5. Summary

The CFQS is the first quasi-axisymmetric stellarator and is now under construction. In order to study the physics related to E_r, poloidal flow, and turbulence transport, HIBP diagnostics are planned and the feasibility of the HIBP in the CFQS is verified in this paper. By calculating the probe orbit in the CFQS in the case of a magnetic field strength of 1.0 T, $^{133}Cs^+$, $^{85}Rb^+$, $^{39}K^+$ are useful if the acceleration voltage is below 200 keV. Observable regions are examined, from center to edge where we can measure potential in plasma. Beam attenuation is estimated for typical plasma parameters. The analysis tells us that the beam decay ratio, I_D/I_0 is 10^{-3} ~ 10^{-2}. $^{133}Cs^+$ for the density range of $\bar{n}_e < 1.0 \times 10^{19}$ m^{-3}, $^{85}Rb^+$ for $\bar{n}_e > 1.0 \times 10^{19}$ m^{-3} are appropriate choices for probe beam ion species in the CFQS.

Acknowledgments

This research is supported by programs of international collaborations with overseas laboratories (UFEX105), promotion of magnetic confinement research using helical devices in Asia (URSX401), the NIFS general collaboration project, NIFS18KBAP041, NIFS20KBAP067, NIFS20KBAE001, and “PLADyS”, Japan Society for the Promotion of Science (JSPS) Core-to-Core Program, A. Advanced Research Networks.

References

[1] F. Wagner et al., *Regime of improved confinement and high beta in neutral-beam heated divertor discharges of the ASDEX Tokamak, Phys. Rev. Lett.* **49** (1982) 1408.

[2] F. Wagner et al., *Development of an edge transport barrier at the H-mode transition of ASDEX, Phys. Rev. Lett.* **53** (1984) 1453.

[3] ASDEX Team, *The H-Mode of ASDEX, Nucl. Fusion* **29** (1989) 1959.

[4] A. Fujisawa et al., *Electron thermal transport barrier and density fluctuation reduction in a toroidal helical plasma, Phys. Rev. Lett.* **82** (1999) 2669.

[5] T. Minami et al., *Transport of the plasma which neoclassical internal transport barrier on CHS, Plasma Phys. Control. Fusion* **44** (2002) A197.

[6] P.H. Diamond et al., *Zonal flows in plasma-a review, Plasma. Phys. Control. Fusion* **47** (2005) R35.

[7] A. Fujisawa et al., *Experimental progress on zonal flow physics in toroidal plasmas, Nucl. Fusion* **47** (2007) S718.

[8] F.C. Jobes and R. L. Hickok, *A direct measurement of plasma space potential, Nucl. Fusion* **10** (1970) 195.

[9] G.A. Hallock et al., *The TMX heavy ion beam probe, IEEE Trans. Plasma Sci.* **22** (1994) 241.

[10] K. Ishii, *Application of a gold neutral beam probe and an end-loss energy component analyzer to space potential measurements in a tandem mirror, IEEE Trans. Plasma Sci*. **22** (1994) 332.

[11] Y. Hamada et al., *Calibration of a heavy ion beam probe for the JIPP T-IIU tokamak by gas puffing, Fusion Eng. Des.* **34-35** (1997) 667.

[12] T. Ido et al., *Heavy ion beam probe diagnostic system on JFT-2M, Rev. Sci. Instrum.* **70** (1999) 955.

[13] A.V. Melnikov et al., *Calibration of the heavy ion beam probe parallel plate analyzer using the gas target and reference beam, Rev. Sci. Instrum.* **68** (1997) 308.

[14] A. Malaquias et al., *Inversion methods for the measurements of MHD-like density fluctuations by Heavy Ion Beam Diagnostic, JINST* **10** (2015) P09024.

[15] D.R. Demers et al., *Heavy ion beam probe advances from the first installation of the diagnostic on an RFP, Rev. Sci. Instrum.* **83** (2012) 10D711.

[16] A. Fujisawa et al., *Active trajectory control for a heavy ion beam probe on the compact helical system, Rev. Sci. Instrum.* **67** (1996) 3099.

[17] I.S. Bondarenko et al., *Installation of the advanced heavy ion beam probing diagnostics on the TJ-II Stellarator, Czech. J. Phys.* **50** (2000) 1397.

[18] A.V. Melnikov et al., *Plasma potential measurements by the heavy ion beam probe diagnostic in fusion plasmas: biasing experiments in the TJ-II stellarator and T-10 tokamak, Fusion Sci. Technol.* 46 (2004) 299.

[19] A.V. Melnikov et al., *Plasma potential evolution study by HIBP diagnostic during NBI experiments in the TJ-II stellarator, Fusion Sci.Technol.* **51** (2007) 31.

[20] T. Ido et al., *6 MeV heavy ion beam probe on the Large Helical Device, Rev. Sci. Instrum.* **77** (2006) 10F523.

[21] T.P. Crowley et al., *Improvement in the spatial resolution of heavy ion beam probe measurements through application of ion optics, Rev. Sci. Instrum.* **92** (2021) 013503.

[22] K. Matsuoka et al., *Post-CHS project, Plasma Physics reports* **23** (1997) 542.

[23] S. Okamura et al., *Physics and engineering design of the low aspect ratio quasi-axisymmetric stellarator CHS-qa, Nucl. Fusion* **41** (2001) 1865.

[24] S. Okamura et al., *Confinement characteristics of the quasi-axisymmetric stellarator CHS-qa, Nucl. Fusion* **44** (2004) 575.

[25] K. Matsuoka et al., *Engineering design study of quasi-axisymmetric stellarator with low aspect ratio, Fusion Science and Technology* **46** (2004) 378.

[26] CFQS TEAM, *NIFS-SWJTU JOINT PROJECT FOR CFQS -PHYSICS AND ENGINEERING DESIGN- VER.3.1, RESEARCH REPORT NIFS-PROC Series: NIFS-PROC-119*, Jan.25, 2021.

[27] A. Shimizu et al., *Configuration property of the Chinese first quasi-axisymmetric stellarator, Plasma and Fusion Research* **13** (2018) 3403123.

[28] H. F. Liu et al., *Magnetic configuration and modular coil design for the Chinese first quasi-axisymmetric stellarator, Plasma and Fusion Research* **13** (2018) 3405067.

[29] M. Isobe et al., *Current status of NIFS-SWJTU joint project for quasi-axisymmetric stellarator CFQS, Plasma and Fusion Research* **14** (2019) 3402074.

[30] H.F. Liu et al., *Configuration characteristics of the Chinese first quasi-axisymmetric stellarator, Nucl. Fusion* **61** (2021) 016014.

[31] M. Drevlak, *Automated optimization of stellarator coils, Fusion Technology* **33** (1998) 106.

[32] G.A. Proca, T. S. Green, *Minimum image size in a parallel plate electrostatic spectrograph, Rev. Sci. Instrum.* **41** (1970) 1778.

[33] A. Fujisawa et al., *Active control of beam trajectories for heavy ion beam probe on helical magnetic configurations, Rev. Sci. Instrum.* **63** (1992) 3694.

[34] W. Lotz, *Electron-impact ionization cross-sections and ionization rate coefficients for atoms and ions, Astrophys. J. Suppl.* **14** (1967) 207.

[35] S. Ohshima et al., *Development of zeolite ion source for beam probe measurements of high temperature plasma, Rev. Sci. Instrum.* **77** (2006) 03B704.